Hurst parameter analysis of radio pulsar timing residuals

X. S. Na,[1]★ N. Wang,[2] J. P. Yuan,[2] Z. Y. Liu,[2] A. Esamdin,[2] J. Pan[3] and R. X. Xu[1]

[1]*School of Physics and State Key Laboratory of Nuclear Physics and Technology, Peking University, Beijing 100871, China*
[2]*Urumqi Observatory, National Astronomical Observatories, 40-5 South Beijing Road, Urumqi 830011, China*
[3]*Purple Mountain Observatory, 2 West Beijing Road, Nanjing 210008, China*

ABSTRACT

We analyse the timing residuals for 50 pulsars observed using the Nanshan 25-m radio telescope at Urumqi Observatory by determining the Hurst parameter for each data set using the rescaled range method. These pulsars have been observed over a time span of 5–8 yr and have been selected to have timing residuals that resemble white noise rather than smooth curves. The results are compared with those for shuffled residual series. Despite the noise-like appearance, some timing residual series showed Hurst parameters that deviated significantly from the shuffled series. We conclude that Hurst parameter analysis is capable of detecting long-term memory in timing residuals.

Key words: methods: statistical – pulsars: general.

1 INTRODUCTION

All pulsars show a remarkable uniformity of rotation rate on a time-scale of a few days, as expected of an isolated spinning body with a large stable moment of inertia (Lyne & Smith 2006). The angular momentum of a radio pulsar is slowly decreasing through the slowdown torque of the magnetic dipole radiation. However, there are some interesting irregularities, such as timing noise (which exhibits itself as low-frequency noise) and glitch events (which are sudden changes in the pulsar spin frequency).

It is anticipated that valuable information regarding many interesting physical processes related to pulsars is coded in the timing residual. Therefore, employing statistical measures to characterize the timing residual is important in the study of pulsars and consequently the properties of matter at supranuclear densities. Efforts to quantify low-frequency timing residuals were made as early as the 1970s. According to random walks of various quantities (Boynton et al. 1972), most current models such as vortex creeping are still restricted to treatment of timing noise only as a random process in certain quantities. One exception was presented by Harding, Shinbrot & Cordes (1990), who analysed timing data of the Vela pulsar to look for evidence of chaotic behaviour using a 'correlation sum' technique to estimate the fractal dimension of the system. In contrast, little attention was paid to higher frequency timing residuals, which after the subtraction of the smooth component look like white noise.

Furthermore, the number of observed pulsars has accumulated to ∼10^3 (Manchester et al. 2005), but the data collected are often incomplete for a conclusive analysis. It is, therefore, crucial to diagnose currently available data even though these are limited in data

span. The results could guide us to concentrate on those pulsars with anomalous timing residuals in future observations. Here, we introduce a statistical method rarely used in time-domain astronomy: Hurst parameter analysis, which is sensitive to any inherent correlation in the time series. Our analysis of the timing data observed by the 25-m radio telescope at Urumqi Observatory for 50 pulsars indicates that Hurst parameter analysis is capable of detecting anomalous signals that disguise themselves as white-noise residuals.

In Section 2 we introduce the Hurst parameter and some other related concepts, then describe a modified rescaled range method to estimate the Hurst parameter for timing residual series with the simple Monte Carlo simulation used in this article. In Section 3 we present the estimated Hurst parameters for 50 selected pulsars. A discussion of the results and conclusion are given in Section 4.

2 HURST PARAMETER ANALYSIS

2.1 Basic concepts

A discrete time series $\{R_t\}$ is called *independently distributed* if two variables in any pair are independent of each other, i.e. covariance $\text{Cov}(R_i, R_j) = 0$ for any $i \neq j$. An independently distributed series is often called *white noise* for its constant power spectrum. A discrete time series is called *stationary* if its probability distribution and correlation structure are constant with respect to time. More strictly speaking, the time series is stationary if, for any d variables picked from the series, the vectors $(R_{k_1}, \ldots, R_{k_d})$ and $(R_{k_1+n}, \ldots, R_{k_d+n})$ have the same n-point distribution (Dieker 2004).

A stationary time series is called *self-similar* if it looks the same after scaling up by a factor. To be more specific, if we sum m consecutive variables $R'_k = \sum_{i=mk}^{m(k+1)-1} R_i$, there exists a scaling function $a(m)$ so that for any d variables from the series $(R_{k_1}, \ldots, R_{k_d})$ the

vectors $(R_{k_1}, \ldots, R_{k_d})$ and $a(m)(R'_{k_1}, \ldots, R'_{k_d})$ have the same n-point distribution (Dieker 2004). Finally, a time series is said to have *Hurst parameter H* if it is stationary, self-similar and have a scaling function $a(m) \propto m^{-H}$ (Hurst 1951). It is easy to see that if we take $\{R_n\}$ as the pace length of a random walk, the newly defined series $\{R'_n\}$ is just the range covered by the m consecutive steps of that random walk.

Independently distributed series have $H = 1/2$. A time series with $H \neq 1/2$ is called *fractal Brownian motion*. The name comes from the fact that the Hurst parameter is related to fractal dimension D of the time series through $D = 2 - H$. For series with $H > 1/2$ the generated random walk will cover a longer range than Brownian motion, implying a positive correlation. For series with $H < 1/2$ the generated random walk will cover a shorter range than Brownian motion, implying a negative correlation or in other words a self-reverting trend; such a series is called an *anti-persistent series*. Therefore, estimation of the Hurst parameter can probe correlation inside a series, i.e. how memory of its past influences its future.

2.2 Calculation methods

Various methods to estimate the Hurst parameter were introduced over the years in the study of long-memory time series. Several of the most widely known methods are the rescaled range method (also known as the *R/S* method), the aggregated variance method, the absolute value of aggregated series method (henceforth called the absolute value method), Higuchi's method, the periodogram method, Peng's method and Whittle's method (for a detailed description of these methods, the reader is referred to Taqqu, Teverovsky & Willinger 1995). In the following calculation, we choose to adopt the rescaled range method[1] modified to account for non-uniformly sampled time series.

In Taqqu et al. (1995) and Rea, Reale & Brown (2009), several widely used methods including the rescaled range method were tested on simulated long-memory series of length $\sim 10^3$–10^4 with known Hurst parameter values (fractal Gaussian noise, ARIMA models and the Campito data). They concluded that the rescaled range method has a small bias in estimating the Hurst parameter, which decreases very slowly with increasing series length. On the other hand it is one of the two best-performing estimators when applied to Campito data and when judged by the Beran test (Beran 1994). In this work we choose the rescaled range method because of two advantages. First, the method gives a more accurate Hurst parameter when estimating series with length less than 1000 than several other methods. Second, it is easy to use and easy to modify for non-uniformly sampled series.

2.3 The rescaled range method

Here we describe the rescaled range method to estimate the Hurst parameter for timing residual series. The validity of this method is based on the theorem by Hurst (1951) and Feller (1951) stating that, for any independent random process with finite variance, the range covered by a random walk divided by the standard deviation has the trend

$$R/S = \sqrt{\frac{\pi\tau}{2}}. \tag{1}$$

To estimate the parameter using the rescaled range method for timing residual record $R_1, R_2, \ldots, R_N$ taken at time $t_1, \ldots, t_N$, we first split this series into n segments of length $\Delta t_n \approx (t_N - t_1)/n$, i.e. $\{R_N\}$ is re-grouped in the following way:

$$R_1, \ldots, R_{\ell_1}; R_{\ell_1+1}, \ldots, R_{\ell_2}; \ldots; R_{\ell_{n-1}+1}, \ldots, X_R,$$

so that

$$t_1 + (i-1)\Delta t \leq t_{\ell_i}, t_{\ell_i+1}, \ldots, t_{\ell_{i+1}-1} < t_1 + i\,\Delta t. \tag{2}$$

For the ith segment $\{R_{\ell_i}, \ldots, R_{\ell_{i+1}-1}\}$ for example, we calculate the average A_i and the standard deviation S_i of the record $\{0, R_{\ell_i+1} - R_{\ell_i}, \ldots, R_{\ell_{i+1}-1} - R_{\ell_i}\}$ to form a new series $\{Y_{\ell_i}, \ldots, Y_{\ell_{i+1}-1}\}$, the elements of which are given by

$$Y_{\ell_i+k} = \frac{1}{S_i}(R_{\ell_i+k} - A_i). \tag{3}$$

The *range* $\tilde{R}_i^{(n)}$ is defined to be the difference between the maximum and the minimum of the accumulated series:

$$Z_k^{(i)} = \sum_{j=1}^{k} Y_{\ell_i+j} \quad (k \leq \ell_{i+1} - \ell_i - 1),$$
$$\tilde{R}_i^{(n)} \equiv \max\left(Z_{k=1,\ldots}^{(i)}\right) - \min\left(Z_{k=1,\ldots}^{(i)}\right), \tag{4}$$

where the superscript n is the number of segments and for each n there is an averaged range

$$\tilde{R}^{(n)} = \frac{1}{n}\sum_{i=1}^{n} \tilde{R}_i^{(n)}. \tag{5}$$

Therefore, for $n = 1, 2, \ldots, n_{\max}$ we obtain a series $\{(\Delta t_n, \tilde{R}^{(n)})\}$. $n_{\max}$ is chosen to be the largest segment number to ensure that every segment contains at least five data points. To estimate the power-law index, we then use linear regression to fit $\{(\log \Delta t_n, \log \tilde{R}^{(n)})\}$ for the slope as an estimation of the Hurst parameter H.

2.4 Simple Monte Carlo simulations

There are two complications when estimating the Hurst parameter using the rescaled range method for actual timing residual data.

(i) The original rescaled range method can only estimate the Hurst parameter for data without errors; however, for pulsar timing, errors in time of arrival are not negligible.

(ii) The formula $(R/S) \sim \tau^{1/2}$ for independent series is only satisfied asymptotically. In fact, comparing the Hurst parameter estimated for a finite series with the exact value 0.5 is inappropriate due to the bias in the rescaled range method mentioned before.

To take error bars into account, we use a simple Monte Carlo simulation. First, generate[2] 1000 series $\{(t_n, R_n)\}$ for each timing residual series, where R_n follows a Gaussian distribution with standard deviation equal to the data error-bar lengths and expectation equal to the centres of the data error bars. Then, the Hurst parameters H of these series are calculated for each residual series, their average and standard deviation being taken as the estimated Hurst parameter and its uncertainty.

In order to make sure that deviation from 0.5 truly represents a persistent or anti-persistent trend, we shuffle the residuals together with their uncertainties ten times (leaving the observation time unchanged) and then calculate the Hurst parameter for these

---

[1] The rescaled range method is the original method to estimate the Hurst parameter by Hurst (1951).

[2] Throughout this paper we use a Mersenne–Twister pseudo-random number generator to generate random numbers.

ten shuffled series using the above method. If, on average, the shuffled residual series have Hurst parameters that are much closer to 0.5, then we can conclude that the deviation in calculated Hurst parameter for residual series truly represents (anti-)persistence of the series, since random shuffling should destroy any memory structure hidden in the series.

Before analysing the result, it is necessary to clarify several issues. First, it is generally believed (Rea et al. 2009) that the rescaled range method has a bias in estimating the Hurst parameter. It was pointed out in very early studies that in practical use the rescaled range method tends to overestimate H for $H < 0.72$ (Mandelbrot & Wallis 1969; Feder 1988). It can be easily shown that several other methods give a more accurate Hurst parameter than the rescaled range method for long time series (with a length of ≥ 1000). For example, for 1000 independent series with length 1000 and following a standard normal distribution, we estimated the Hurst parameters using the aggregated variance, absolute value and rescaled range methods and obtained $H = 0.564 \pm 0.048$, 0.494 ± 0.055 and 0.487 ± 0.060 respectively. Because of this effect, our method of comparing shuffled and unshuffled series is only capable of confirming persistence with a Hurst parameter significantly larger than 0.5. On the other hand, the aggregated variance and absolute value methods give a much less accurate Hurst parameter estimation for short series, especially short series with non-uniform sampling. For example, we produced 1500 series of length 300 with randomly distributed sample spacing (spacings are taken to follow the absolute value of a normal distribution with mean 10 and standard deviation 10, which resembles a pulsar timing residual series) and estimated the Hurst parameters for these series using the modified rescaled range method and aggregated variance and absolute value methods modified similarly to the procedure in Section 2.3. The distributions of the estimated Hurst parameters are shown in Fig. 1. Mean Hurst estimations for the aggregated variance and absolute value methods are 0.29 and 0.43 with standard deviations of 0.26 and 0.19 respectively. As we can see from Fig. 1, the distributions of Hurst
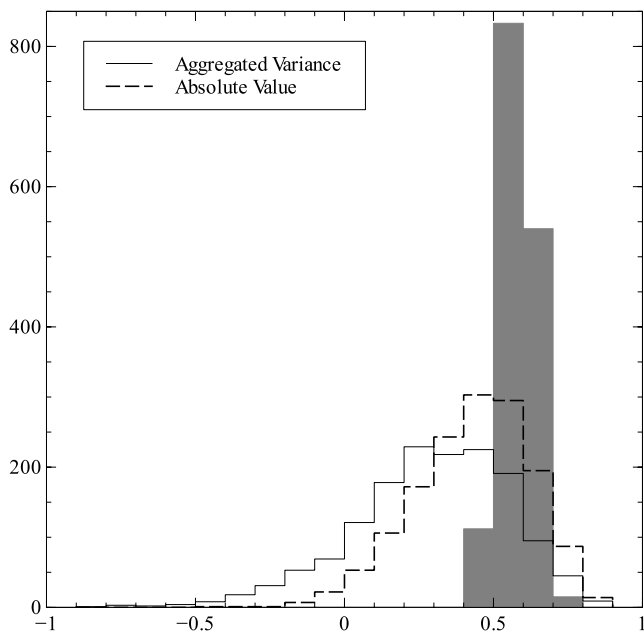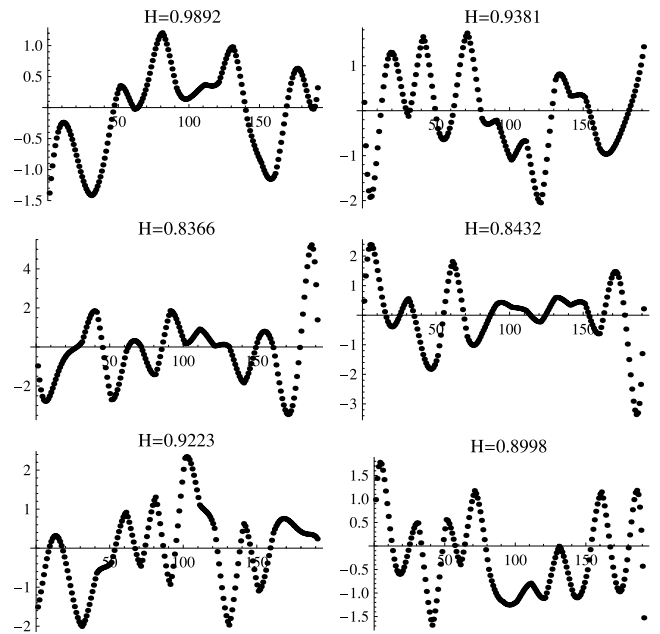
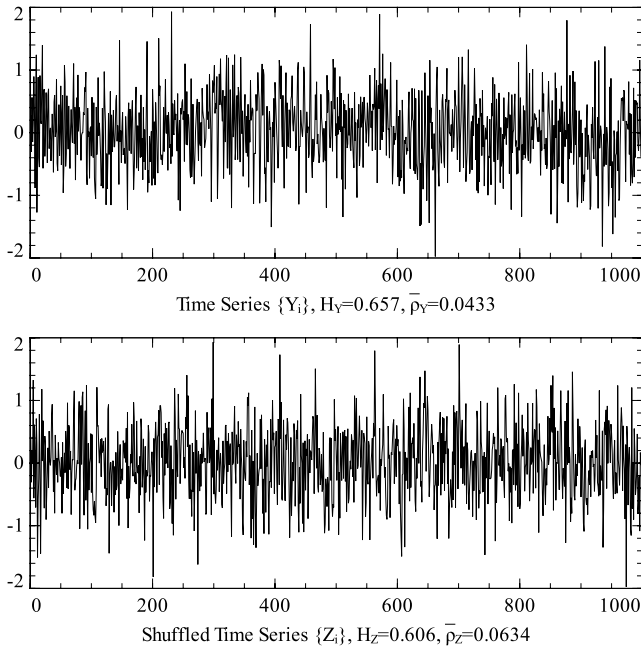**Figure 2.** Hurst parameters of six smooth-curve series similar to timing noise.

estimations for aggregated variance and absolute value methods are quite dispersed, while the rescaled range method gives a much more concentrated distribution with $H = 0.581 \pm 0.055$. This is the reason we chose the rescaled range method for estimating the Hurst parameter in this work.

A second issue is that timing noise with a smooth appearance will yield a trivial Hurst parameter $H \sim 1$. This can be easily understood through the relation with fractal dimension $D = 2 - H$. To illustrate this effect we generate six series of 20 random numbers and interpolate each series to obtain a polynomial. Next we sample these smooth polynomials with a frequency ten times higher. The estimated Hurst parameters, together with sampled data points of a smooth curve, are shown in Fig. 2. As we can see, all Hurst parameters are near 1. Since the low-frequency component dominates, these six series have very strong correlation between consecutive data points and this makes the length covered by accumulated random walks increase almost linearly with time on small scales. In this case, Hurst parameter analysis provides no more information than one can see with the naked eye. Hence Hurst parameter analysis can only be used on timing residuals with a white-noise appearance.

The last issue is that Hurst parameter analysis is capable of detecting long-term memory, while simpler methods to explore dependence such as an adjacent pair-correlation sum are unable to detect such a feature. To illustrate this capability we generate a time series with vanishing correlation between adjacent data points but with a correlation length of 10 data points with the following steps.

(i) Generate 1000 random numbers (standard normal distribution) $X_1, \ldots, X_{1000}$.
(ii) Define a new series $\{Y_i\}$ with $Y_i = X_i$ for $i = 1, \ldots, 10$, and $Y_i = (X_{i-10} + X_i)/2$ for $i = 11, \ldots, 1000$.
(iii) Shuffle the time series $\{Y_i\}$ to obtain $\{Z_i\}$.

The two time series $\{Y_i\}$ and $\{Z_i\}$ are shown in Fig. 3. The time series $\{Y_i\}$ by definition has no correlation between adjacent variables at all but has correlation length $= 10$, while $\{Z_i\}$ should be an independent series. The Hurst parameters for the two series estimated by the rescaled range method are $H_Y = 0.657$ and $H_Z = 0.606$

Figure 1. Distribution of Hurst parameters estimated by various methods for 1500 series of length 300 with randomly distributed sample spacings. The solid line, dashed line and shaded distributions are given by the aggregate variance, absolute value and rescaled range methods, respectively.

Figure 3. A simulated time series with correlation length = 10 and the shuffled series together with their Hurst parameters (estimated by the rescaled range method) and average correlations between adjacent values.

respectively. On the other hand, the average Pearson's correlations between adjacent values are $\bar{\rho}_Y = 0.0433$ and $\bar{\rho}_Z = 0.0634$ respectively, which shows no significant difference.

3 TIMING RESIDUAL DATA ANALYSIS

3.1 The sample of observed timing residuals

Data analysed in this work consist of 5–8 yr of timing residual data from the Nanshan 25-m radio telescope at Urumqi Observatory. Timing data are processed using the standard pulsar software packages PSRCHIVE (Hotan, van Straten & Manchester 2004) and TEMPO2 (Hobbs, Edwards & Manchester 2006) to obtain timing residuals. The times of arrivals (TOA) of radio pulses are fitted using PSRCHIVE software from observation data by an input-accumulated pulse profile. The TEMPO2 software uses coordinate-system conversion parameters that account for various effects (Roemer delay, Einstein delay, Shapiro delay, etc.) and pulsar parameters (P, $\dot{P}$, etc.) to establish a model to predict the arrival time of pulses. The timing residual is obtained as the difference between the observation and this timing model. We then used the `splk` package of TEMPO2 to output timing residuals with error bars in units of seconds at each TOA. We select 50 pulsars among those regularly monitored at Nanshan with a central radio frequency (RF) of 1540 MHz and total bandwidth of 320 MHz (Wang et al. 2001). For a certain pulsar, its timing observation is made about once per ten days. The standard of selection is a large signal-to-noise ratio profile and large mean flux at 1400 MHz, residuals resembling white noise and with no recognizable glitch. Basic parameters of selected pulsars (P, $\dot{P}$, dispersion measure DM and degree of linear polarization) from the ATNF Pulsar Catalogue (Manchester et al. 2005) and EPN data archive are also listed in Table 1.

3.2 Results and analysis

Using the above methods, Hurst parameters H for timing residual series and H' for shuffled series of the selected 50 radio pulsars are calculated, together with uncertainties estimated by the simple Monte Carlo method explained in the above section. The results are listed in Table 1 together with the basic parameters of the corresponding pulsars. The distribution of Hurst parameters of residual series is shown in Fig. 4. Fig. 5 shows a comparison between the Hurst parameters before and after shuffling: Hurst parameters after shuffling are all near 0.5 and are plotted as a connected error-bar band.

From Figs 4 and 5 we see that data length and non-uniformity have only a limited effect on the value of shuffled Hurst parameters, since they are all near 0.5. On the other hand, several pulsars do show Hurst parameters that differ significantly from the shuffled values.

From these results, we can see that most Hurst parameters for pulsar timing residuals are concentrated around ∼0.5–0.6. However, there are some Hurst parameters far away from the shuffled series. For PSRs J0612+3721, J1136+1551, J1847−0402, J2048−1616 and J2354+6155 the calculated Hurst parameter average is $H \geq 0.72$ and, as is shown in Fig. 5, the Hurst parameters drop toward 0.5 significantly after shuffling, indicating strong persistence, and the error bars of Hurst values before and after shuffling are far apart. As mentioned in Section 2.4, the rescaled range method tends to overestimate series with Hurst parameter <0.72, therefore these Hurst parameter values are less likely to be overestimated to such a high level. On the other hand, for PSRs J0055+5117, J0134−2937, J2308+5547 and J2326+6113 the calculated Hurst parameter values $H \leq 0.45$; these increase significantly after shuffling, indicating considerable anti-persistence, and the error bars before and after shuffling do not overlap.

In Fig. 6 we select three pulsars to illustrate typical persistent and anti-persistent timing residual series: PSR J0055+5117 with $H = 0.36(2)$ and $H' = 0.55(8)$ representing anti-persistent series, PSR J2108+4441 with $H = 0.55(3)$ and $H' = 0.61(5)$ representing independent series and PSR J2354+6155 with $H = 0.74(3)$ and $H' = 0.57(4)$ representing persistent series.

4 DISCUSSION AND CONCLUSION

We calculated the Hurst parameter using the rescaled range method for timing residual series of 50 radio pulsars with white-noise-like timing residuals obtained from the Nanshan telescope and compared the result with that of shuffled series. Most of the pulsars from our selection have Hurst parameters that do not differ much from the shuffled values. However, we found several pulsars (some showing a persistent trend and a few showing an anti-persistent trend) with interesting Hurst parameters despite having white-noise-like timing residuals. Comparison with Hurst parameters after shuffling confirms that these trends cannot be attributed to finite-length effects or uncertainties in the timing residual. This shows that our algorithm is capable of detecting hidden correlation in apparently noise-like timing residuals. We therefore suggest that these pulsars be monitored continually to confirm or disprove long-term memory and search for the possible physical process behind such a correlation.

Regarding the selection, we picked 50 pulsars with a large mean flux at 1400 MHz and large signal-to-noise ratio profile that have white-noise-like timing residuals without any trends visible to the naked eye. We are not attempting to perform correlation between the Hurst parameter and other pulsar properties or obtain statistics

Table 1. Basic parameters of the selected 50 pulsars from the ATNF Pulsar Catalog Manchester et al. (2005), together with Hurst parameters for the timing residuals before and after shuffling estimated by the rescaled range method, denoted by H and H' respectively. Degrees of linear polarization $\langle L \rangle/\langle I \rangle$ at 1400 and 1600 MHz are taken from Gould & Lyne (1998) except for J0134−2937, J0215+6218, J1741−3927. For J1741−3927 $\langle L \rangle/\langle I \rangle = 11$ per cent at 1560 MHz according to Wu et al. (1993).

| No.	PSR	P (s)	$\dot{P}$ (10^{-16})	DM (cm$^{-3}\cdot$pc)	$\langle L \rangle/\langle I \rangle$(per cent) 1.4 GHz	1.6 GHz	H	H'
1	J0034−0721	0.9430	4.082	11.38	5	13	0.52(4)	0.56(8)
2	J0055+5117	2.1152	95.38	44.13	27	38	0.36(2)	0.55(8)
3	J0134−2937	0.1370	0.7837	21.81	–	–	0.45(4)	0.63(11)
4	J0141+6009	1.2229	3.911	34.80	20	21	0.51(3)	0.58(4)
5	J0152−1637	0.8327	12.99	11.92	18	–	0.58(7)	0.57(8)
6	J0215+6218	0.5489	6.621	84.00	–	–	0.58(5)	0.56(6)
7	J0304+1932	1.3876	12.95	15.74	5	7	0.55(6)	0.58(8)
8	J0502+4654	0.6386	55.82	42.19	2	12	0.66(4)	0.56(6)
9	J0525+1115	0.3544	0.7361	79.35	7	12	0.53(7)	0.6(7)
10	J0601−0527	0.3960	13.02	80.54	27	31	0.5(4)	0.53(8)
11	J0612+3721	0.2980	0.5947	27.14	8	19	0.76(3)	0.57(7)
12	J0814+7429	1.2922	1.681	6.116	31	36	0.57(3)	0.55(6)
13	J0820−1350	1.2381	21.05	40.94	6	7	0.55(5)	0.56(6)
14	J0837+0610	1.2738	67.99	12.89	4	12	0.6(5)	0.56(6)
15	J0846−3533	1.1161	16.01	94.16	–	23	0.59(2)	0.59(6)
16	J0908−1739	0.4016	6.695	15.89	6	10	0.54(4)	0.59(6)
17	J0943+1631	1.0874	0.9109	20.32	7	29	0.51(7)	0.56(9)
18	J1041−1942	1.3864	9.449	33.78	3	3	0.54(9)	0.56(11)
19	J1115+5030	1.6564	24.93	9.195	14	28	0.57(7)	0.57(10)
20	J1136+1551	1.1879	37.34	4.864	9	16	0.79(3)	0.57(5)
21	J1239+2453	1.3824	9.600	9.242	35	33	0.59(5)	0.55(6)
22	Jp1257−1027	0.6173	3.627	29.63	27	32	0.57(6)	0.58(8)
23	J1543+0929	0.7484	4.325	35.24	12	5	0.58(3)	0.57(7)
24	J1703−3241	1.2118	6.598	110.3	–	–	0.6(4)	0.58(6)
25	J1733−2228	0.8717	0.4270	41.14	11	9	0.51(5)	0.59(8)
26	J1741−0840	2.0431	22.75	74.90	11	19	0.46(8)	0.59(11)
27	J1741−3927	0.5122	19.31	158.5	–	–	0.69(3)	0.58(6)
28	J1750−3157	0.9104	1.965	206.3	21	–	0.58(5)	0.57(11)
29	J1807−0847	0.1637	0.2880	112.4	5	10	0.65(5)	0.55(7)
30	J1822−2256	1.8743	13.54	121.2	18	15	0.64(3)	0.64(7)
31	J1823+0550	0.7529	2.267	66.78	11	10	0.56(8)	0.57(9)
32	J1837−0653	1.9058	7.720	316.1	19	40	0.56(3)	0.56(8)
33	J1840+5640	1.6529	14.95	26.70	31	18	0.55(4)	0.58(5)
34	J1847−0402	0.5978	517.1	141.98	8	17	0.79(3)	0.56(6)
35	J1900−2600	0.6122	2.045	37.99	11	17	0.49(6)	0.56(7)
36	J1921+2153	1.3373	13.48	12.46	3	9	0.58(4)	0.58(5)
37	J1946+1805	0.4406	0.2409	16.22	28	28	0.5(4)	0.57(7)
38	J1954+2923	0.4267	0.01711	7.932	24	12	0.45(10)	0.59(11)
39	J1955+5059	0.5189	13.72	31.97	10	12	0.64(5)	0.58(5)
40	J2002+4050	0.9051	17.39	131.3	4	9	0.54(4)	0.57(5)
41	J2013+3845	0.2302	88.51	238.2	66	64	0.54(3)	0.59(7)
42	J2018+2839	0.5580	1.481	14.17	5	7	0.65(5)	0.56(5)
43	J2048−1616	1.9616	109.6	11.46	21	18	0.73(6)	0.57(7)
44	J2108+4441	0.4149	0.8621	139.8	10	12	0.55(3)	0.61(5)
45	J2113+4644	1.0147	7.146	141.3	19	24	0.62(3)	0.57(6)
46	J2157+4017	1.5253	34.33	70.86	18	24	0.66(3)	0.56(4)
47	J2308+5547	0.4751	1.995	46.54	4	15	0.45(4)	0.58(9)
48	J2321+6024	2.2565	70.37	94.59	19	17	0.63(4)	0.55(5)
49	J2326+6113	0.2337	3.526	122.6	11	18	0.47(4)	0.55(5)
50	J2354+6155	0.9448	162.6	94.66	19	16	0.74(3)	0.57(4)

of Hurst parameter values for a large population, since our selection may be biased. Our method is aimed at finding the possibility that timing noise resembling white noise is not really an independent random series. As is well known, many pulsars have rather smooth timing residuals commonly known as timing noise. These residual series would yield quite large Hurst parameters, as is shown in Section 2.4, because smooth curves have trivial fractal dimensions.

It should also be mentioned that TOA are obtained using the Nanshan telescope, which receives two linear polarizations, but the two channels are not calibrated before summing to form the total
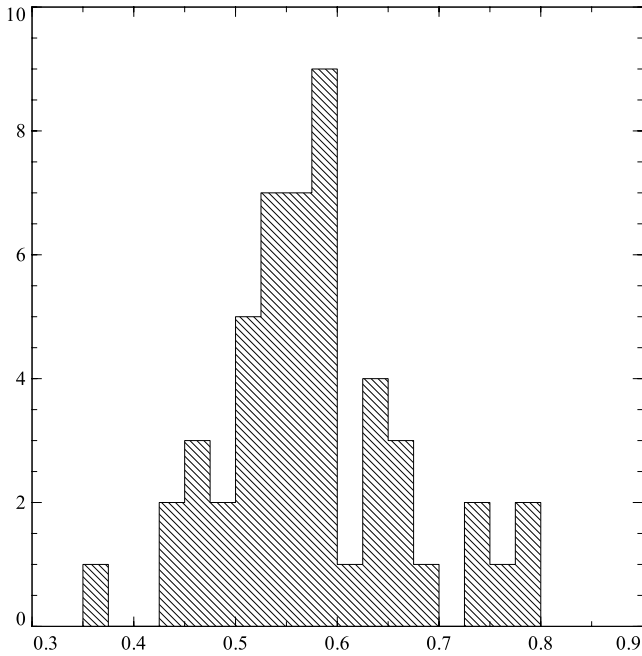
**Figure 4.** Distribution of Hurst parameters for the 50 selected pulsars.
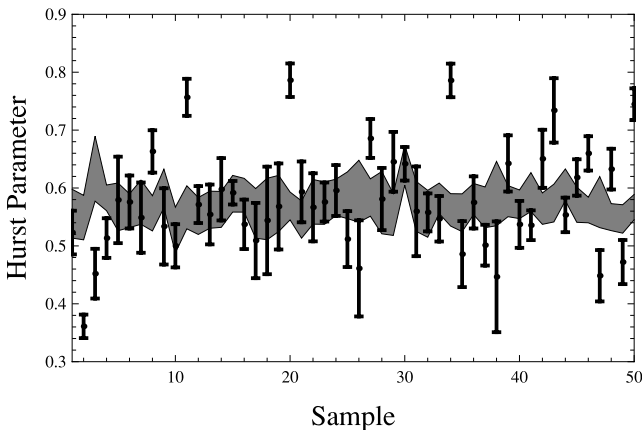
Figure 5. Hurst parameters of 50 pulsar timing residual series. Black dots with error bars are Hurst parameters for each pulsars timing residual series. The grey band is connected by error bars of shuffled residual series of the same pulsar. The order of the pulsars is the same as in Table 1.

intensity. There can be a parallactic effect, which might possibly create dependence in residual series for pulsars with high linear polarization if the gains of the two channels are not well-matched. Its size depends on the mismatch of the gains and the degree and form of the linear polarization, but should only be a small fraction ($\lesssim 0.1$) of the pulse width even if the gains differ by 1–2 dB. We list the degree of linear polarization $\langle L \rangle / \langle I \rangle$ at 1400 and 1600 MHz for most of the selected 50 pulsars in Table 1, where $L = (Q^2 + U^2)^{1/2}$. We plot the Hurst parameter against $\langle L \rangle / \langle I \rangle$ in Fig. 7 and, as we can see, there is no clear dependence of the Hurst parameter on the degree of linear polarization.

There are various physical processes that might be responsible for the long-term memory of the pulsar timing residual. These can be classified into three groups:

(i) processes from the interior of the neutron star, i.e. due to the fluctuation of internal (e.g. microquakes due to the partial release
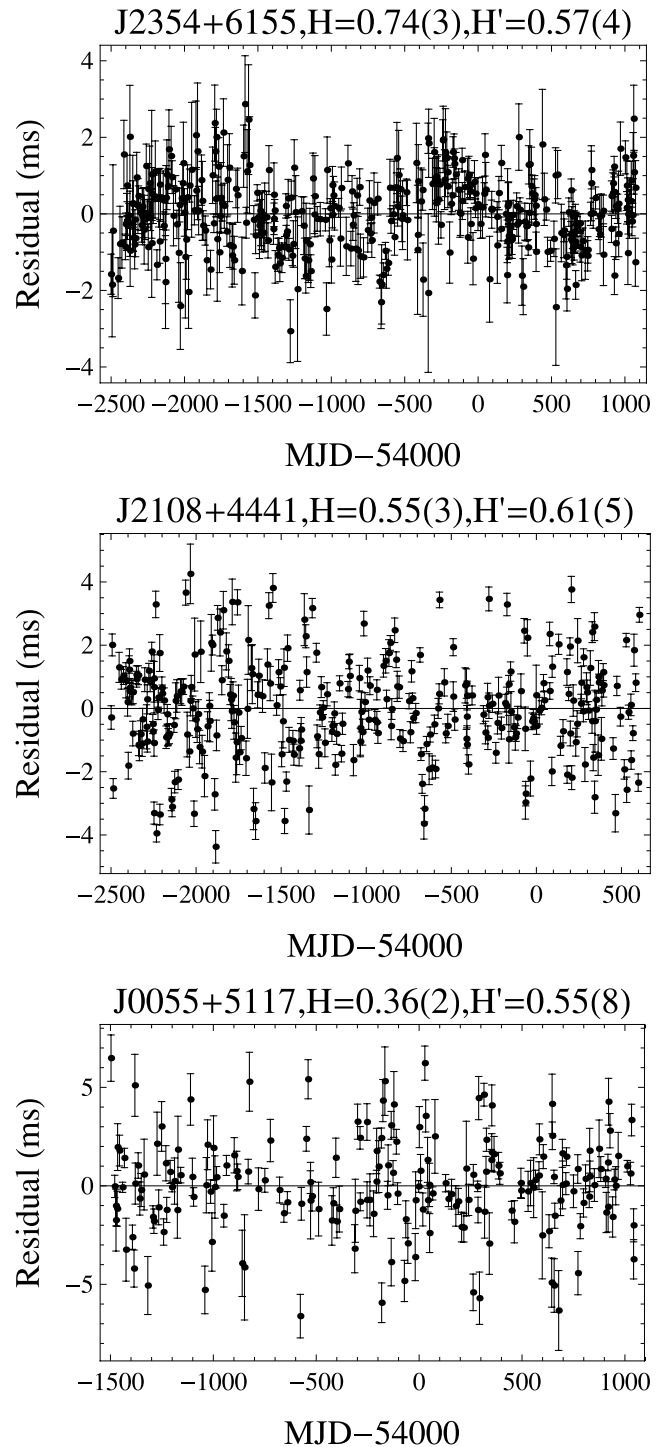
Figure 6. Representative timing residuals. Top: PSR J0055+5117 representing an anti-persistent series; middle: PSR J2108+4441 representing an independent series; bottom: PSR J2354+6155 representing a persistent series.

of elastic energy (Pines & Shaham 1972) and random pinning and unpinning of vortex lines (Packard 1972; Anderson & Itoh 1975)) and external (e.g. accretion flow; Lamb, Pines & Shaham 1978) torques;

(ii) emission processes (e.g. magnetospheric activity; Cheng 1987);
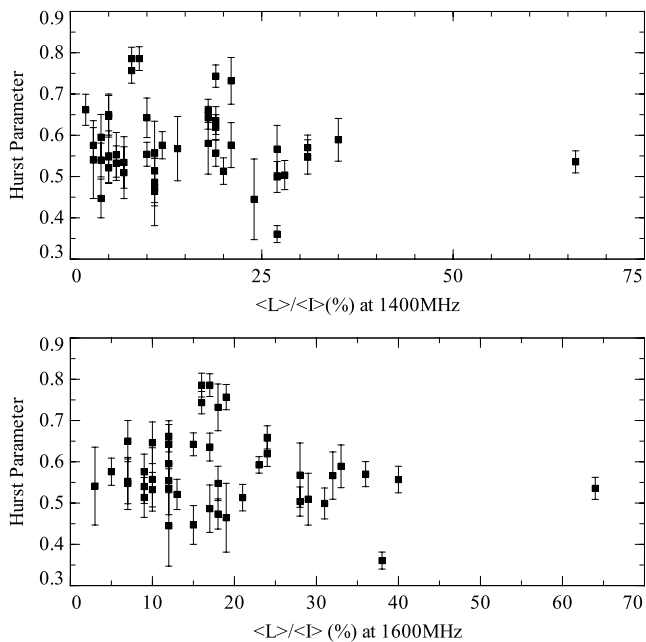
Figure 7. The Hurst parameter against the degree of linear polarization at 1400 and 1600 MHz. All pulsars in our selection except for four have data covering at least one of these two wavelengths. See Table 1.

(iii) processes arising from the propagation of radio emission (e.g. dispersion-measure variations and gravitational waves).

For the last class of origin, it has long been proposed that the timing residual can be used to set upper limits on gravitational waves (Bertotti, Carr & Rees 1983) and that, given enough time, pulsar timing arrays might be the first equipment to detect gravitational waves directly (Manchester 2006). Most of these previous works predict uncorrelated randomness or random walks in certain quantities, while the Hurst parameter may be capable of uncovering richer dependent structure that is hidden in the timing residual. The physical origin that leads to dependent series is much more limited than that of uncorrelated random fluctuations. Therefore, long-term memory detected by the Hurst parameter may reveal more detailed information about the physical origin of the timing residual. For instance, it has been proposed that under certain conditions Euler equations for rotating objects with magnetic dipole moment misaligned with the rotation axis would show chaotic spin-down behaviour (see Harding et al. 1990). Chaotic behaviour may lead to an interesting Hurst parameter, since it is essentially dependent.

Lastly, our choice of estimator is based on the fact that available timing residual records are limited in length. With the accumulation of timing data we will have long enough timing residual series to adopt the unbiased algorithms mentioned in Section 2.2 with better convergence, and therefore obtain much more information on the hidden long memory of timing residuals. Therefore, we expect that the application of the Hurst parameter to timing residuals of longer time-span can provide more information about pulsar origin.

REFERENCES

Anderson P. W., Itoh N., 1975, Nat, 256, 25
Beran J., 1994, Statistics for Long Memory Processes. Chapman & Hall/CRC Press, New York
Bertotti B., Carr B. J., Rees M. J., 1983, MNRAS, 203, 945
Boynton P. E., Groth E. J., Hutchinson D. P., Nanos G. P., Partridge R. B., Wilkinson D. T., 1972, ApJ, 175, 217
Cheng K. S., 1987, ApJ, 321, 799
Dieker T., 2004, Master's thesis, Vrije Univ. Amsterdam
Feder J., 1988, Fractals. Plenum Press, New York
Feller W., 1951, Ann. Math. Stat.,, 22, 427
Gould D. M., Lyne A. G., 1998, MNRAS, 301, 235
Harding A. K., Shinbrot T., Cordes J. M., 1990, ApJ, 353, 588
Hobbs G. M., Edwards R. T., Manchester R. N., 2006, MNRAS, 369, 655
Hotan A. W., van Straten W., Manchester R. N., 2004, PASA, 21, 302
Hurst H. E., 1951, Trans. Amer. Soc. Civil Eng., 116, 770
Lamb F. K., Pines D., Shaham J., 1978, ApJ, 224, 969
Lyne A. G., Smith F. G., 2006, Pulsar Astronomy. Cambridge Univ. Press, Cambridge, p. 74
Manchester R. N., 2006, Chin. J. Astron. Astrophys., 6, 139
Manchester R. N., Hobbs G. B., Teoh A., Hobbs M., 2005, AJ, 129, 1993
Mandelbrot B. B., Wallis J. R., 1969, Water Resour. Res., 5, 321
Packard R. E., 1972, Phys. Rev. Lett., 28, 1080
Pines D., Shaham J., 1972, Nat, 235, 43
Rea W., Reale M., Brown J., 2009, preprint (arXiv:0901.0762)
Taqqu M. S., Teverovsky V., Willinger W., 1995, Fractals, 3, 785
Wang N., Manchester R. N., Zhang J., Wu X. J., Yusup A., Lyne A. G., Cheng K. S., Chen M. Z., 2001, MNRAS, 328, 855
Wu X., Manchester R. N., Lyne A. G., Qiao G., 1993, MNRAS, 261, 630

This paper has been typeset from a TEX/LATEX file prepared by the author.